Supplementary Information for

Thermal Conductivity Switching in $Sm_{1-x}Gd_xS$ over a Broad Temperature Window via a Pressure-induced, Thermally Revertible Hysteretic Phase Transition

Ankita Saha,[1] *Yudan Li,*[2] *Chuting Cai,*[3] *Li Shi,*[2,3] *Joshua E. Goldberger*[1,]*

[1]Department of Chemistry and Biochemistry, The Ohio State University, Columbus, OH, USA

[2]Walker Department of Mechanical Engineering, The University of Texas at Austin, Austin, Texas 78712, USA

[3]Materials Science and Engineering Program, The University of Texas at Austin, Austin, Texas 78712, USA

*Goldberger.4@osu.edu

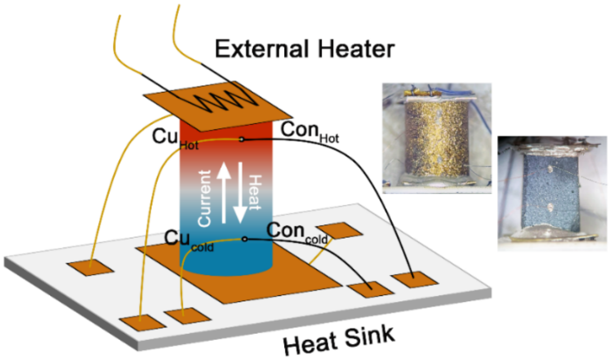

Figure S1. (Left) Schematic Diagram of a steady state heater-sink measurement setup with (right) images of prepared devices.

Measurement Uncertainties

Resistivity:

The general formula for evaluating the error in the resistivity measurements takes the form,

$$\rho_{error} = \sqrt{\left(\frac{50nV}{V_{Sample}}\right)^2 + \left(\frac{dL}{L}\right)^2 + \left(\frac{dW}{W}\right)^2 + \left(\frac{dTh}{Th}\right)^2}$$

Here V_{sample} denotes the voltage measured across the sample while dL, dW, and dTh represent the uncertainties in the sample length (defined by the thermocouple separation), width, and the thickness that is the dimension on the sample face containing the thermocouples. The measured voltage across the sample is generally much larger than the uncertainty in the nanovoltmeter; however, uncertainties arising from sample geometry contribute errors of about 8-15% for each relevant dimension.

Thermal Conductivity:

The general formula for estimating the error in the thermal conductivity measurements takes the form,

$$\kappa_{error} = \sqrt{\left(\frac{50nV}{V_{Cold}}\right)^2 + \left(\frac{50nV}{V_{Hot}}\right)^2 + \left(\frac{dL}{L}\right)^2 + \left(\frac{dW}{W}\right)^2 + \left(\frac{dTh}{Th}\right)^2}$$

Here V_{Hot} and V_{Cold} denote the hot and cold side thermocouple voltage, respectively and the same geometric uncertainties described above apply. Again, the voltages are substantially larger than the nanovolt uncertainty. However, the same geometric variances associated with the relative uncertainty in thermal conductivity is often comparable to that of the resistivity measurements that act on the thermal conductivity as well. Consequently, the relative uncertainty in thermal conductivity is often comparable to that of the resistivity.

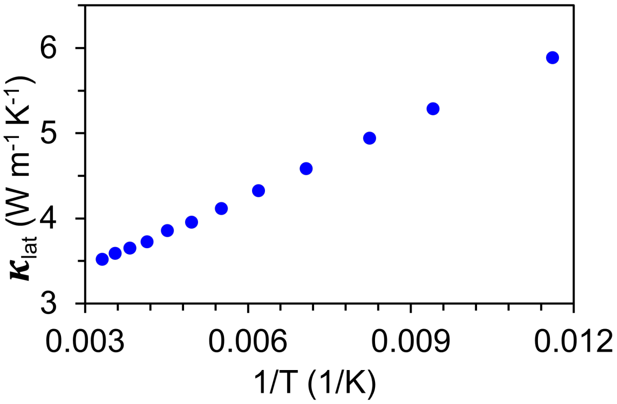

Figure S2. κ_{lat} of the semiconducting SmS phase plotted as a function of 1/T showing a characteristic linear 1/T dependence from 80-300 K

.

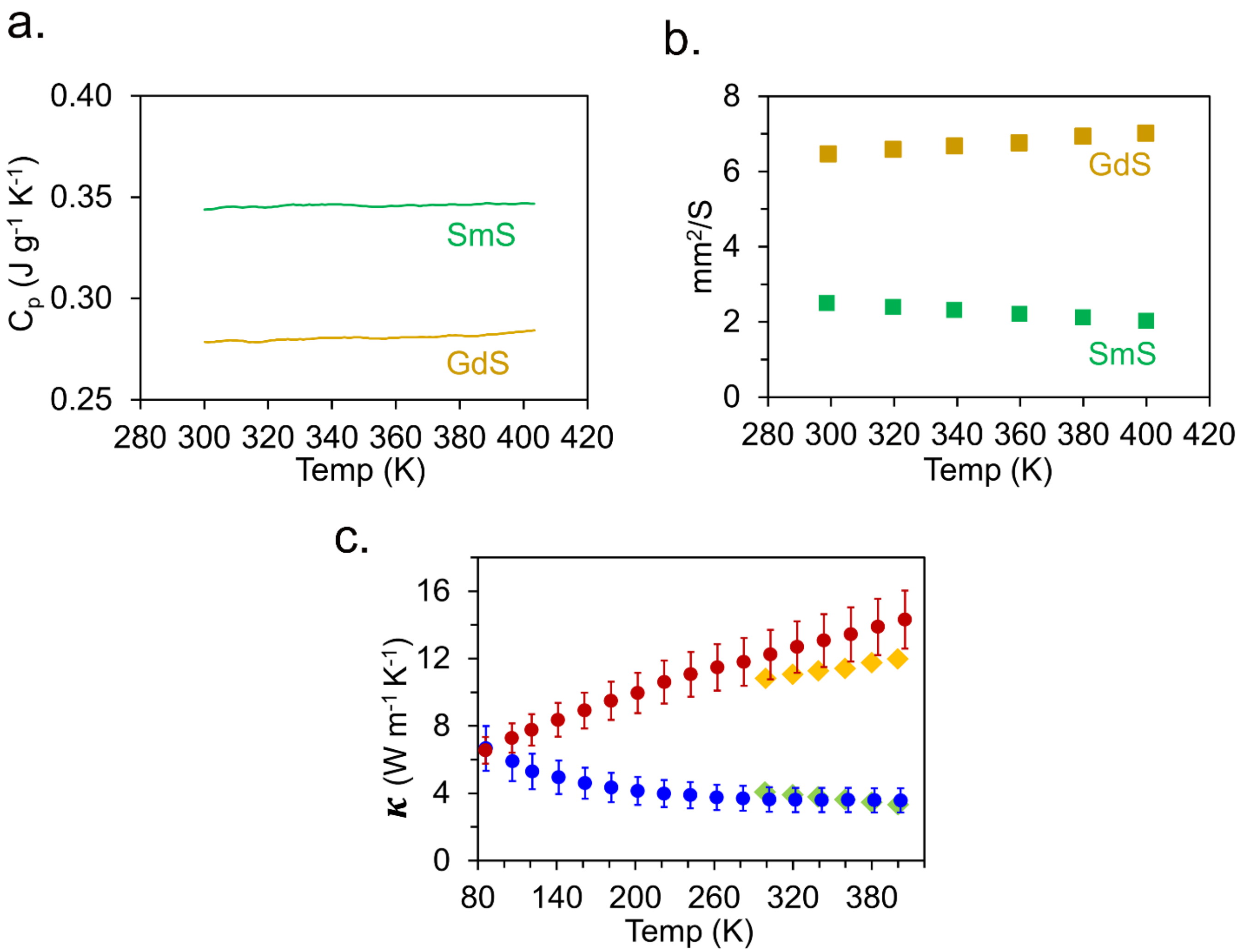

Figure S3. a) Specific heat of SmS (green) and GdS (gold) from 300 – 400 K. b) Thermal diffusivity of SmS (green) and GdS (blue) measured via laser flash analysis. c) Thermal conductivities of SmS (green diamond) and GdS (yellow diamond), derived from the laser flash diffusivity measurements from 300 – 400 K compared to the thermal conductivities of SmS (blue circles) and GdS (red circles) obtained by the classical heater-and-sink method.

The thermal diffusivity is a measure of transient heat-flow and is defined as the thermal conductivity, divided by the product of the specific heat, CP, times the density, ρ. Thermal diffusivity (mm^2/s) was measured by the laser flash analysis (LFA) method (Figure S2). The density of the pellet (g m^{-3}), the diffusivity, and the specific heat (J g^{-1} K^{-1}) were used to calculate the thermal conductivity (W m^{-1} K^{-1}) of SmS (yellow diamonds) and GdS (green diamonds).

$$\alpha = \frac{\boldsymbol{\kappa}}{\rho C_P}$$

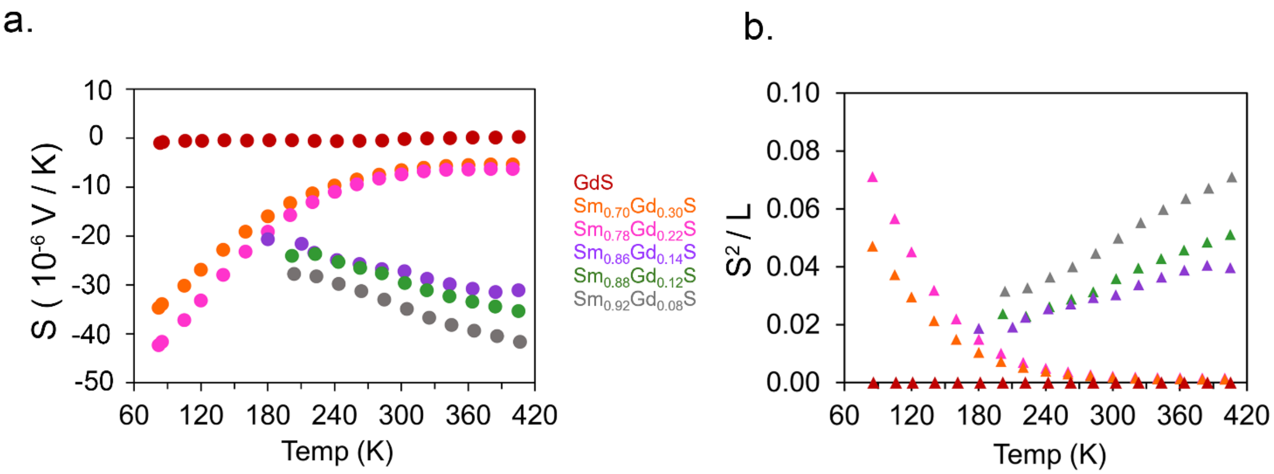

Figure S4 a) Measured Seebeck coefficient of $Sm_{1-x}Gd_xS$ (0.08 ≤x≤ 0.30) and GdS from 85K to 400 K. b) S^2/L of the $Sm_{1-x}Gd_xS$ (0.08 ≤x≤ 0.30) and GdS samples from 85K to 400 K. The small value of <0.07 indicates that there are minimal correlation effects and that the standard Lorentz number approximation is valid.

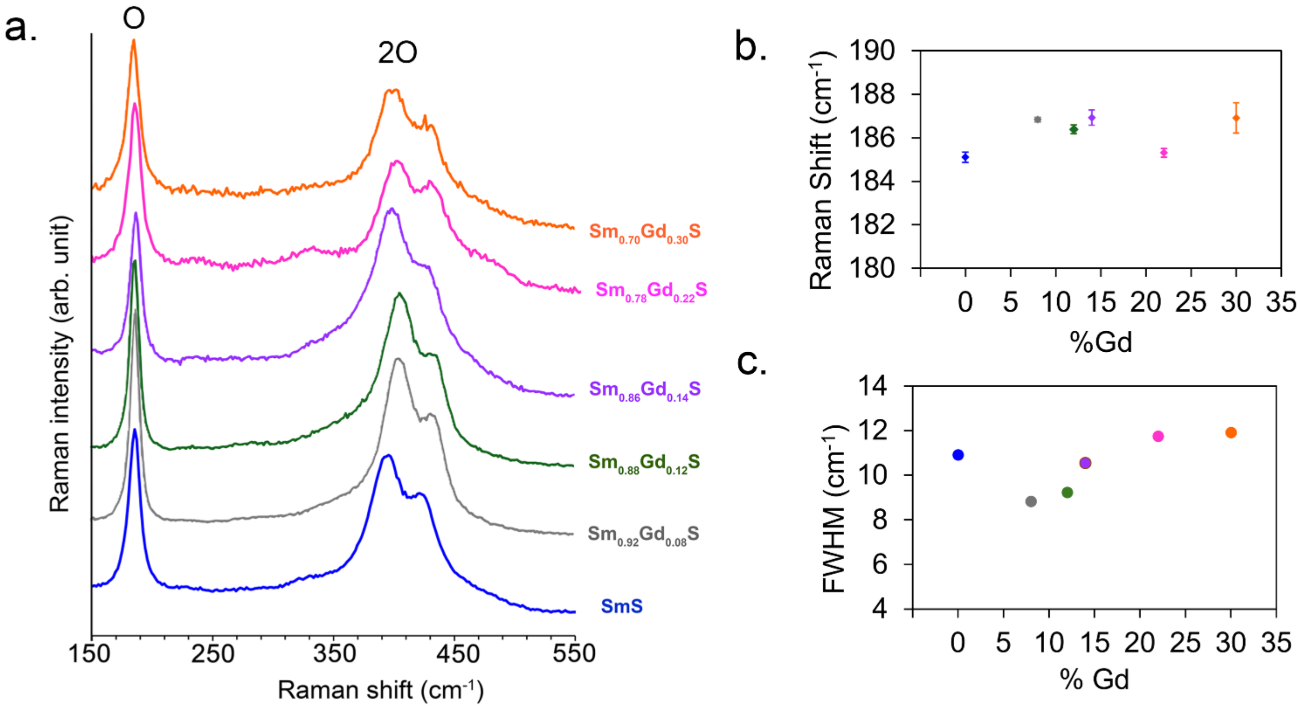

Figure S5. a) The Raman spectra of $Sm_{1-x}Gd_xS$ ($0.0 \leq x \leq 0.3$) excited using λ=514 nm, showing the first order optical mode at 185-187 cm^{-1}, and second order modes from 380-440 cm^{-1}. b) The Raman shift of the first order optical mode as a function of Gd stoichiometry. c) The Full-Width at Half Maximum (FWHM) of the first order optical mode as a function of Gd stoichiometry.

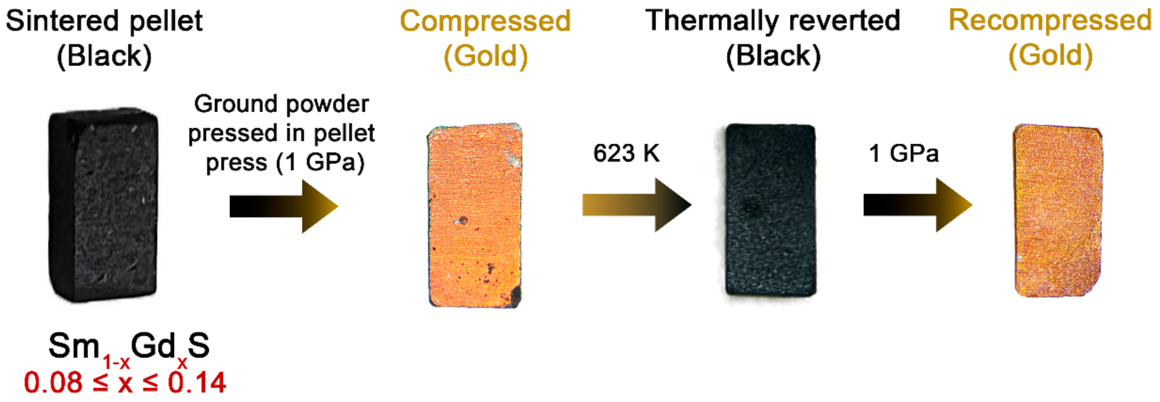

Figure S6. Photographic images showing the change in color of the $Sm_{1-x}Gd_xS$ alloys as they are compressed into the gold phase, thermally reverted into the black phase, and recompressed into the gold phase.

Preparation of pellets for thermal conductivity measurements

"Sintered" - The thermal conductivity was first measured for 1600°C sintered pellets of $Sm_{1-x}Gd_xS$. These pellets were in the black phase for $0.08 \le x \le 0.14$ and in the gold phase for $x=0.30$

"Compressed" - The sintered pellets were then ground into powder and uniaxially compressed using a rectangular 6 × 3 mm pellet die. A force corresponding to a pressure of 1 GPa was applied for 60 s, producing copper-colored gold-phase pellets. The resulting rectangular compressed pellets had thicknesses of ~0.5 mm and lateral dimensions of 3 mm × 6 mm and were used to fabricate devices for thermal conductivity measurements (Figure 3a).

“Thermally reverted” - After measuring the thermal conductivity of the compressed gold phase over the temperature range 220-400 K, the sample was heat-treated in an argon atmosphere for 5-15 s, (supplementary video), resulting in a thermally reverted black-phase. Devices were fabricated from this reverted phase, and thermal conductivity measurements were performed over the same temperature range.

“Recompressed” - Thermally reverted sample was ground up and then recompressed in a pellet press under similar conditions (1 GPa, 60s), yielding a recompressed gold-phase pellet which was subsequently used for analogous thermal conductivity measurements.

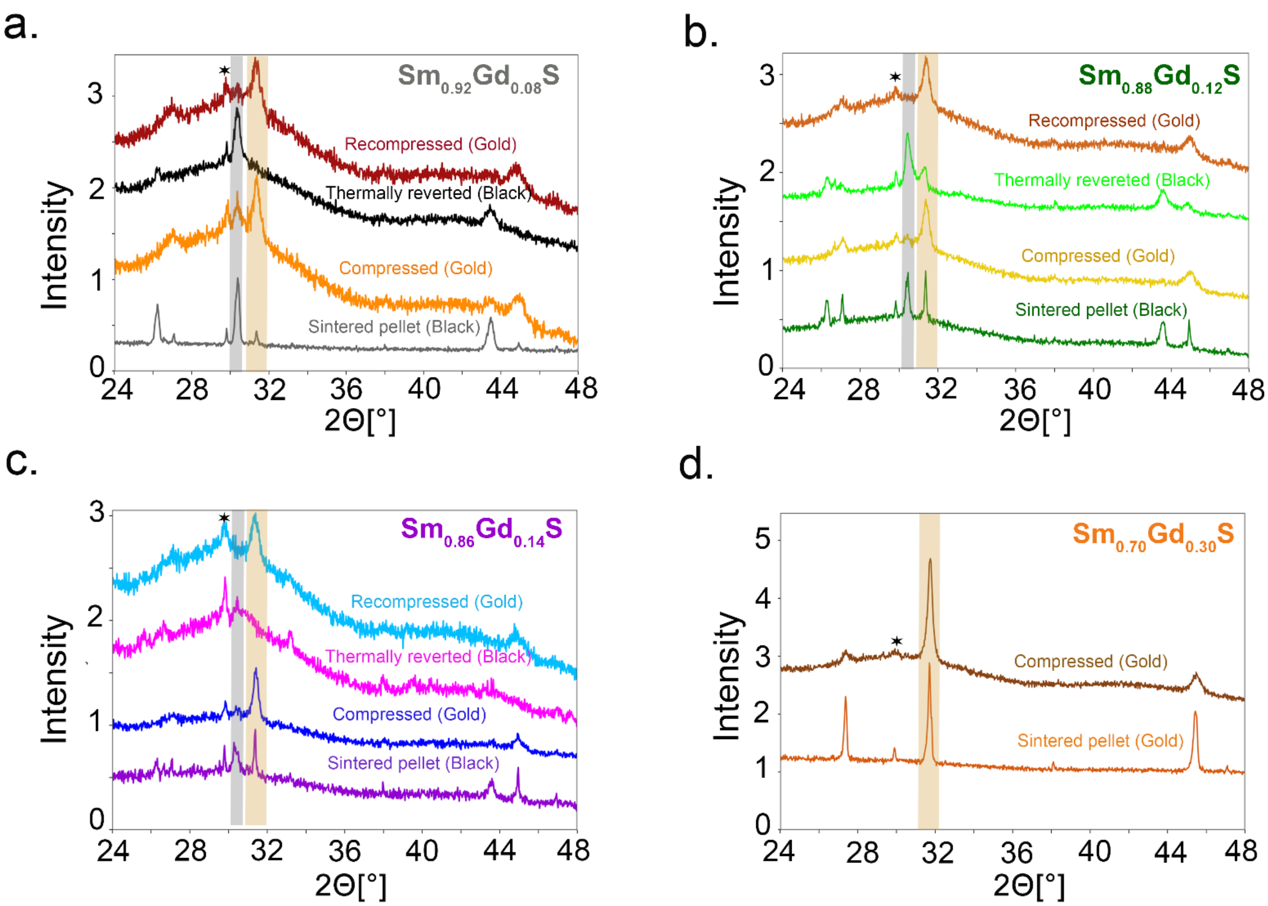

Figure S7. XRD of sintered pellet-black phase, compressed-gold phase, thermally reverted- black phase and recompressed- gold phase of stoichiometries a) $Sm_{0.92}Gd_{0.08}S$, b) $Sm_{0.88}Gd_{0.12}S$, c) $Sm_{0.86}Gd_{0.14}S$, d) $Sm_{0.70}Gd_{0.30}S$. In all XRD patterns, the most intense peak of the larger unit cell black phase is highlighted grey, the smaller unit cell gold phase is highlighted orange and the $(Sm_{1-x}Gd_x)_2O_2S$ impurities are starred.

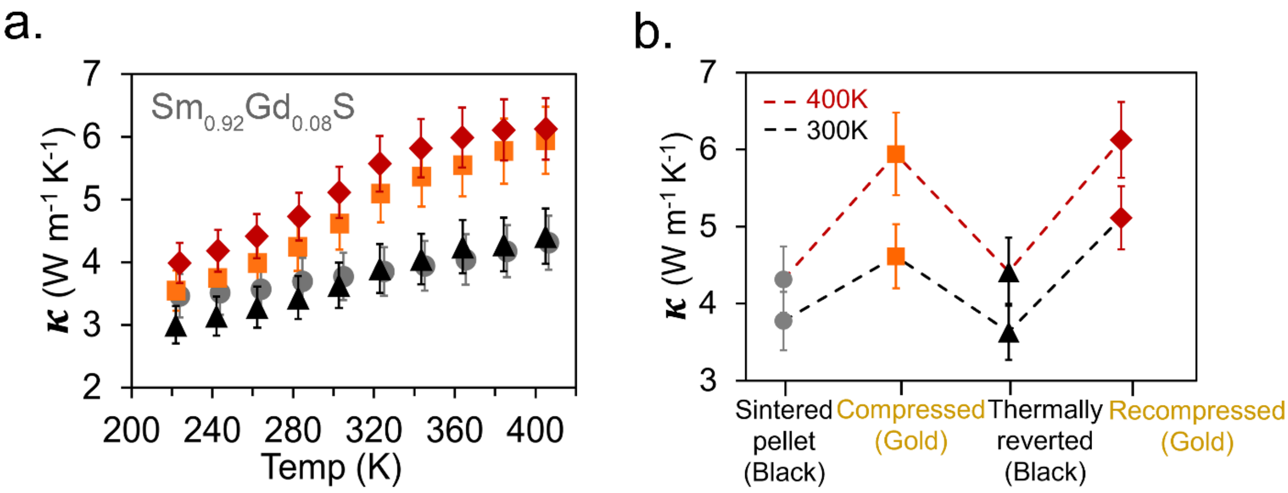

Figure S8. Thermal conductivity switching of $Sm_{0.92}Gd_{0.08}S$. a) Thermal conductivity vs. Temperature of the as-grown sintered pellet, compressed, annealed, and re-compressed samples. b) The thermal conductivity after these triggers at 300 K (black dashed line) and 400 K (red dashed line). In a and b, the gray circles correspond to the sintered pellet-black phase, the orange squares correspond to the compressed-gold phase, the black triangles correspond to the thermally reverted-black phase, and the red diamonds correspond to the recompressed-gold phase measurements.

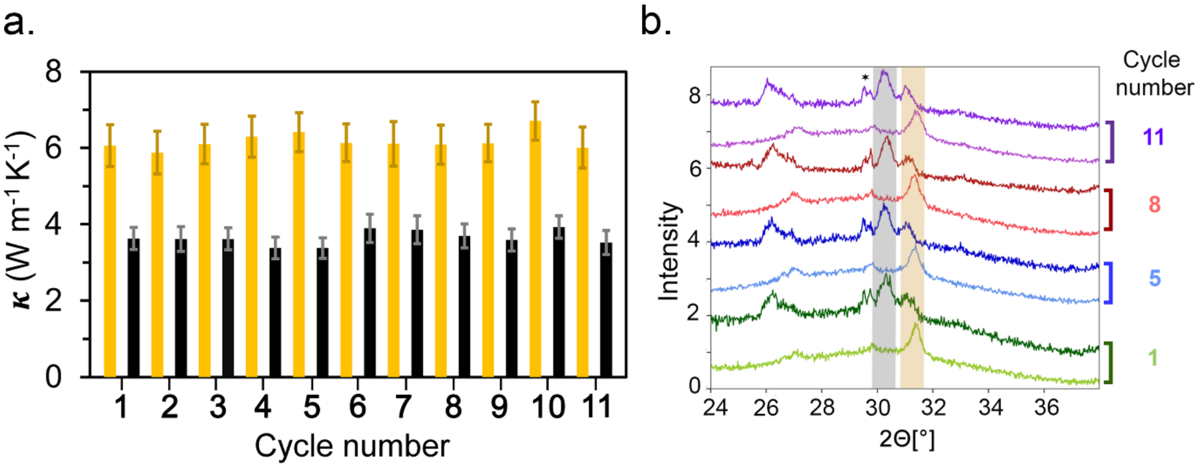

Figure S9. a) Measured 400 K thermal conductivity of a single $Sm_{0.88}Gd_{0.12}S$ pellet after repeated cycles of uniaxial compression (gold) and thermal reversion (black). One compression-thermal reversion sequence is defined as one cycle. The measured thermal conductivities of the gold phases formed after uniaxial compression are within errors of each other as are those of the black phases after thermally reverting, even after 10 consecutive cycles. b) XRDs of compression (gold) and thermal reversion (black) of cycle number 1, 5, 8 and 11. In all XRD patterns, the most intense (200) reflections of the larger unit cell black phase is highlighted grey, the smaller unit cell gold phase is highlighted in orange and the $(Sm_{1-x}Gd_x)_2O_2S$ impurity reflections are starred.

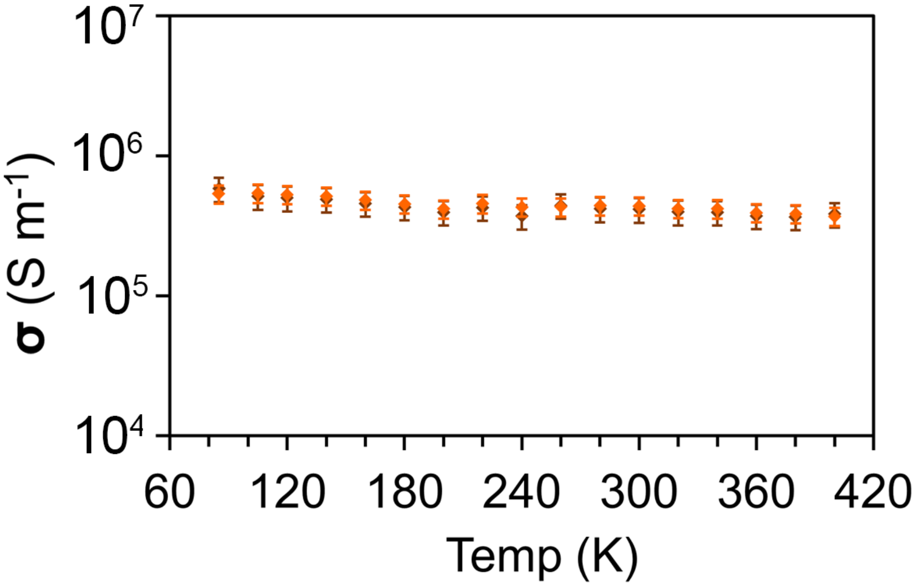

Figure S10. The measured electrical conductivity of the non-switching $Sm_{0.70}Gd_{0.30}S$ pure metallic phase, measured before (orange) and after 1 GPa compression (brown). There is a negligible change in electrical conductivity as a function of pressure.